Controlled growth of metal nanoparticles on atomically thin 2D insulator and conductive films and their role in surface catalytic reactions

Detailed final report

Representative members of two-dimensional (2D) graphene-like materials are boron nitride (BN) and graphene. In the framework of the project, we first focused on the preparation and characterization of the BN layer. BN growth was examined on Rh(111) surface, which was our choice as a substrate among other possibilities (Cu(111), Au(111)), which are also suitable for the in situ growth of hexagonal boron nitride (h-BN). Rh(111) surface offers the possibility of creating a periodically corrugated and nanostructured (so-called "nanomesh") h-BN structure that could open new technological routes to create further promising nanostructures. The BN layer was formed by the decomposition of borazine ($B_3N_3H_6$) based on literature data. Characteristic Auger transitions of B and N appeared in the Auger spectra at kinetic energies of 175 and 384 eV, indicating that borazine bonded to the surface. The gradual thermal decomposition of borazine and the formation of the BN layer were monitored by thermal desorption mass spectroscopy (TDS), electron and ion spectroscopic methods (AES, HREEL, XPS, LEIS) and scanning tunneling microscopy (STM). During heating of the borazine-saturated surface (TDS), the physisorbed borazin molecule was desorbed at a peak temperature of 176 K. At higher temperatures, only molecular hydrogen (H_2) desorption was found. The characteristic H_2 desorption peak at 310 K was followed by an elongated desorption range of approx. up to 800 K. The process can be described by the following equations:

$$B_3N_3H_{6\ (a)} \rightarrow B_3N_3H_{6-n\ (a)} + nH_{\ (a)}\ (1);$$

$$B_3N_3H_{6-n\ (a)} \rightarrow BN + H_{\ (a)}\ (2);$$

$$H_{\ (a)} + H_{\ (a)} \rightarrow H_{2\ (g)}\ (3).$$
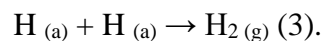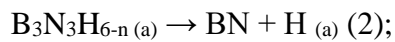
CO adsorption was not observed after borazine treatment described above, from which it was concluded that each Rh site are covered in the outermost surface layer. Two characteristic loss peaks appeared at 790 and 1510 cm^{-1}. The higher energy peak belongs to the longitudinal optical phonon contribution of the h-BN layer, while the other vibration peak belongs to the transverse optical phonon mode.

Since literature data about h-BN on alloy surfaces is very scarce, in the present project Au-Rh bimetallic surfaces were also investigated in h-BN formation process. In our previous detailed studies about the thermal behavior of Au adsorbed on the Rh(111) surface, it was found that two fundamentally different morphological states can be produced: (1) deposition of gold (submonolayer quantity) at 500 K produced gold islands with monolayer thickness on the

Rh(111) atomic terraces, on the other hand one atomic thick Au islands, elongated towards the direction of atomic Rh steps, are also formed; (2) if this surface was heated above at least 700 K, Au-Rh surface alloy was formed. In the frame of the present project the interaction of the Rh-Au alloy surfaces with borazine during h-BN preparation was investigated in detail. It was found that the nanomesh morphology for h-BN/Rh(111) changes sensitively with the pre-alloyed Au. Interestingly, up to relatively large gold coverages (0.9 ML), the nanomesh is present.

As a next step, our goal was to map the morphological and electrical properties of the metal nanoparticles formed (1) on Rh(111) supported h-BN nanomesh and (2) intercalated between the Rh (111) surface and h-BN layer. On the one hand, we studied the growth and thermal properties of Au (or Rh) evaporated on the h-BN supported by Rh(111). On the other hand, the formation of h-BN was studied on Au-Rh alloy surfaces. The surface alloy formed by heating the deposited gold layer on Rh(111) up to 1000 K. Low-energy ion scattering spectroscopy (LEIS), X-ray photoelectron spectroscopy (XPS) and scanning tunneling microscopy (STM) measurements have shown that evaporation of gold on h-BN/Rh(111) at 300 K produces mainly 3D nanoparticles at higher coverages, while at small coverages (<0.2 ML) mainly 2D nanocrystallites are formed. Upon stepwise heating to higher temperatures, gold starts to migrate between the boron nitride monolayer and Rh(111), completed up to 1050 K. In addition, agglomeration and desorption of Au were also observed. Interestingly, the nanomesh structure was retained even above a relatively large amount of gold intercalation. The reverse preparation experiments, in which Au-Rh alloy was formed first and the BN layer was prepared by the high-temperature decomposition of borazine proved that on Rh atoms the BN film forms at a significantly lower exposure than on Au atoms. The nanomesh structure was present up to ~ 0.9 monolayer gold coverage with a smaller pore diameter, however, it gradually disappeared at higher (around 2 ML) Au content. In this way, the use of surface alloys as a support can be an efficient tool for tailoring the mesh structure. DFT theoretical calculations also confirmed the decrease of pore diameter of the BN layer with increasing Au content of the Rh-Au alloy surface.

We also carried out experimental studies related to the interaction of h-BN with deposited Au and Rh, to reveal differences between the two metals. After deposition of Au on h-BN/Rh(111) at 300 K followed by annealing at 1050-1100 K, even for large amounts of Au (~20 ML), it intercalates below the h-BN layer, leaving no Au on the outermost atomic layer, as indicated by LEIS measurements. XPS results disclosed that a (minor) part of Au desorbed from the surface upon annealing. Conversely, repeating the same experiments depositing Rh on h-

BN/Rh(111), the thermally induced intercalation of Rh was only complete for Rh coverages of 5 ML. h-BN in contact with Rh decomposes at and above 1150 K, while the thermal stability of h-BN in contact with Au is clearly higher (decomposes only above 1200 K). This behavior is reasonable considering the more inert character of Au compared to Rh.

In addition to the morphology of gold nanoclusters, their adsorption properties were also investigated by AES, HREELS, and TPD methods. Acetaldehyde reactions were monitored on the Au/Rh(111) surface alloy and on the Au/h-BN/Rh(111) surface layer too. The surface alloy - formed on clean rhodium - did not completely inhibit the surface adsorption of acetaldehyde, however, the bimetallic (surface alloy) structure influenced the dissociation of acetaldehyde, namely, the formation of carbon monoxide was inhibited by the gold domains. We observed that the surface alloy, at higher gold coverages, almost completely eliminates CO formation.

Our results after adsorption of acetaldehyde on the Au/h-BN/Rh(111) system also corroborates the above results, in the absence of suitable adsorption binding sites no CO is formed, no acetaldehyde dissociation process occurred. However, with increasing Au coverage, the amount of acetaldehyde adsorbed on the surface increased. The amount of adsorbed acetaldehyde shows saturation with a certain amount of surface gold on the h-BN/Rh(111) surface, although the Au layer is not yet continuous. This suggests that the active sites are atoms located at the edges of the gold clusters. Furthermore, at low gold coverages, charge transfer processes between substrate Rh and surface gold can be expected, which is likely to cause the presence of negatively charged gold particles, thus enhancing the reactivity of Au/h-BN/Rh(111). The modest reactivity of acetaldehyde on the Au/h-BN/Rh(111) system also significantly influences the decomposition mechanism of ethanol on the same surface. It was concluded that the tendency of acetaldehyde to polymerize on the formed layers is very small due to the lack of strong interaction with the surface. Only traces of acetaldehyde oligomerization were observed on gold decorated pure Rh(111) terraces.

Taking into account that the h-BN monolayer bound to the Rh(111) surface is characterized by a periodically undulating structure ("nanomesh"), it is not only suitable for the monodisperse and uniformly distributed formation of metal nanoclusters, but also capable for ordered adsorption by "trapping" molecules. Accordingly, our plan included for the last years in this field the study of the adsorption of different molecules (ethanol and azobenzene) in the h-BN/Rh(111) system.

Through deposition onto the periodic surface of h-BN we can adjust these parameters of gold thereby we are able to influence the catalytic activity of the nanoparticles. In the next step of our adsorption study, we followed the decomposition of ethanol on gold nanoparticles

supported on 2D h-BN layer prepared on Rh(111). We were able to study the ethanol-gold interaction on the relatively inert boron nitride layer without the so-called "carrier effect" well known from the oxide supports. HREELS and TPD methods have been used on the experimental side. Ethanol showed enhanced stability on Au/h-BN/Rh(111) system. The stabilization effect increases with gold coverage and saturates before gold reaches a continuous adlayer. High selectivity was observed towards "CO free" hydrogen, a small part of ethanol dissociated to hydrogen and acetaldehyde without further decomposition. The experiments also confirmed that the h-BN monolayer thought to be inert was also involved in the dissociation processes in gold as a reaction partner / adsorption center. Density functional theory (DFT) calculations delivered important information about the adsorption characteristics of ethanol and hydrogen on model Au/h-BN/Rh(111). The importance of low-coordinated negatively charged Au atoms is confirmed by DFT results.

We continued our experiments with adsorption studies in the direction of another potential application of h-BN as a template. In this manner the adsorption properties of azobenzene, the prototypical molecular switch, were investigated on the nanomesh prepared on Rh(111), applying TPD and HREELS. TPD studies revealed that azobenzene molecules located on the "wire" and "pore" regions desorb at slightly different temperatures. In our work, determination of the adsorption geometry of azobenzene was top priority, as the adsorption geometry can be crucial in the field of designing surface bound molecular switches. Angle-resolved HREELS measurements demonstrated that the first molecular layer is characterized predominantly by an adsorption geometry with the molecular plane parallel to the surface. STM measurements indicated a clear preference for adsorption in the pores, manifesting a templating effect. DFT calculations confirmed the experimental findings that the molecules adsorb with the phenyl rings parallel to the surface, preferentially in the pores. Laser experiments were performed as well to determine the stability of the h-BN template, since it is essential in the molecular switching measurements that none of the other components (above the investigated molecule) allowed to alter by light exposure. We have found that the 2D structure is not damaged, so h-BN provides an excellent basis for performing azobenzene molecular switching due to its stability as well as inertness.

In connection with the preparation of sandwich-like heterostructures (graphene/BN) we followed also the adsorption properties of benzene (cyclohexene) on h-BN/Rh(111). Based on our Auger electron spectroscopic, high-resolution electron energy loss spectroscopic and mass spectrometry results we can declare that after adsorption of benzene at high temperature we

developed a graphene-like carbon structure on the surface of h-BN/Rh(111) without the removal or destruction of the h-BN film.

The STM studies on h-BN /Rh(111) system were extended, somewhat differently from previous plans, towards the disintegration of the continuous h-BN layer by low-energy (0.5 keV) Ar^+ bombardment and the formation of separate h-BN nanoflakes. This method opens the possibility of preparation of graphene on the rhodium sites created by punching the h-BN sheet. We successfully produced an in-plane BN/graphene monolayer heterostructure.

Concerning the synthesis side of this project, boron nitride (BN) nanoparticles were successfully prepared by CVD method. The boron source was trimethyl borate and NH_3 was used as the precursor for nitrogen component. The reaction conditions (reaction temperature, reaction time, and the flow rate of gases) were systematically adjusted. Ball and wire nanoparticles were obtained with 20, 50, and 110 nm sizes. Monodisperse, regular ball-shape nanoparticles were prepared at the optimal parameter. Colloidal stability was investigated for medical biology and catalytic purposes.

A parallel research direction was to investigate the formation of metal layers/clusters on the oxide single crystal surface to start the initial investigations of the formation of the TiO_2/metal thin film/h-BN structure. As part of the latter experiments, we investigated Au-Pd bimetallic nanoparticles on TiO_2(110) too. We studied two cases in detail, where the amount of Au is smaller and higher compared to the Pd content. This was achieved by evaporating on the surface of the pure oxide support at room temperature 1 ML gold layer in the first case (a) to the 5 monolayer (ML) Pd layers and in the second case (b) 2 ML Au layers onto 3 ML Pd layers. By gradually heating the bimetallic so prepared sandwich structure separate bimetallic Au-Pd nanocrystallites were formed. Our most important finding from our AES, LEED and STM measurements was that the ordered decorative $TiO_{1.2}$ ultrathin film formed on the particles can be controlled by the amount of Au, i.e., the decorative oxide film is formed in the first case (a) but not in the second case (b). This is of great importance in catalysis, as the efficiency of bimetallic catalysts depends largely on the tendency of the metal particles to decorate. An important part of our publication was the study of the structure of Au doped on decorative $TiO_{1.2}$ film. We found that, similarly to the results of our previous studies on the Au-Rh system, we obtained a definite indication for the nano-template effect, ie the control of nucleation of Au particles by the lateral hexagonal periodicity of the $TiO_{1.2}$ film (approximately 1.5 nm lattice constant).

In our parallel studies towards other - non BN related – nanomaterials, the geometric and electrical properties of the atomically thin Nishiyama-Wassermann (NW) Rh layer were characterized by density functional theory (DFT) calculations on Mo(110) surface. We distinguished between the "strain" and "ligand" effects in the Rh film, which were accompanied with 0.11 eV and 0.18 eV shift of the average value (d-band center) of the total d-band density of states (DOS) towards lower energies. The adsorption energy of CO on the NW Rh layer is about 65% of the value calculated for the Rh(111) surface, which opens new reaction pathways for the CO molecule on the Rh film supported on molybdenum. The charge transitions accompanying CO adsorption and the changes in local DOS were modeled. Results highlighted on the mechanism of CO bonding and the factors determining reduced adsorption energy on the bimetallic surface. The effect of Mo doping on the reactions of CO on the Rh surface was also studied. We produced Rh nanoparticles on the $Ti_{1-x}Mo_xO_2$ (x <0.1) film which was formed previously on TiO_2(110) and we observed that mainly MoO_x diffused to the surface of Rh nanoparticles below 500 K and TiO_x particles diffused above it.

MoOx resulted the formation of a new associative CO desorption state (β-CO) after CO adsorption with a peak desorption temperature of 700 K, which is 100 K lower than in the presence of TiOx. This means a reduced activation energy of the C(a) and O(a) recombination reaction and allows a higher reaction rate. The amount of β-CO at 0.2-0.3 monolayer (MR) Mo coverage gives a maximum, which is assigned to the catalytic activity of the MoOx-Rh interface. We have shown that the threshold of Rh coverage required for the appearance of the β-CO state is 0.5-0.7 MR. This was related to the electrical and structural properties of the surface. We found that pure Mo metal (0.2-2.0 MR) promotes the dissociation of CO on 1 MR Rh through the formation of the MoO_zC_y-Rh interface. The molecular adsorption of CO decreases inversely with the MoOx concentration, so to maintain and maximize catalytic activity, MoOx coverage should be kept below 0.5 MR.

The reactions of H_2O, H_2, D_2, and CO gases on pure and Rh-covered plated black titania (BT) are related to industrially important hydrogenation and water gas reactions. BT has a narrower band gap compared to the stoichiometric titanium dioxide and is therefore a promising material for utilization of the energy of visible light. The complex interactions with the above gases were studied by TDS, AES, and sensitive work function measurements. We found that water creates molecular and dissociative adsorption states on the reduced TiO_2(110) surface, and in their dipole layer the positive charges are located on the vacuum side. We have shown that on the highly reduced surface of sr-TiO_2(110) some of the H atoms from the dissociation

of OH species dissolve in titanium dioxide at 200-500 K and then desorb in the form of H_2O at high temperatures.

TiO$_x$ films with less than monolayer coverage formed on Rh particles supported on r-TiO$_2$(110) suppress hydrogen adsorption after stepwise heating but do not prevent diffusion to the support. To elucidate the elemental processes, we examined the co-adsorption of H_2, H_2O and CO on the Rh covered r-TiO$_2$(110) surfaces. We found that on the room temperature CO saturated Rh surface at 330 K, hydrogen is not able to adsorb and therefore cannot migrate to the support either.

In our further adsorption experiments, the studies aimed at a deeper understanding of the elementary steps of the catalytic hydrogenation of CO on the reduced TiO$_2$(110) surface covered with Rh nanoparticles. Since the hydrogenation of CO leads to the formation of water, the interaction of CO and H_2O with the TiO$_x$ layer formed on Rh clusters was also studied. The Rh-TiOx interface showed high reactivity towards both molecules, which was manifested in their dissociation. Furthermore, we proved that the so-called hydrogen spillover process, i.e. the migration of hydrogen atoms from Rh nanoparticles to titanium dioxide, which is important for hydrogen storage and detection processes, does not stop until the metal surface is completely covered with carbon monoxide or with TiOx layer produced after annealing. To optimize the hydrogen spillover, the presence of these adsorbates should be minimized. For a deeper interpretation of the experimental results, DFT calculations were also performed in the framework of Argentine cooperation. The aim of the studies was to determine the stability of the one monolayer thin TiO$_x$ structures on the Rh (111) surface; the calculations showed a good agreement with the experimental results.

We were able to incorporate nitrogen atoms with nitrogen and ammonia plasma into the titanate lattice, during which we were able to change the morphological and optical properties of the titanate nanotube. Subsequently, the modified titanate is subjected to a photochemical test.

Titanium and titanate were used as supports for gold particles with nano and even smaller sizes. We were able to stabilize gold nanoparticles and Au$^+$ ions incorporated in the ion exchange position in the titanate nanotube. The Au/titanate has been shown to be an excellent catalyst in the photocatalytic conversion of methane. The main product in the conversion of methane was hydrogen, in the production of which gold nanoclusters (Au$_{25}$) most likely played a direct role. As a new result, we found that Au nanoparticles supported on titanate nanotubes showed significant activity in CO_2 hydrogenation processes. There was a significant difference between the results collected in the dark experiments (373-873 K) and in the composition of the products

obtained during illumination. At higher temperatures only CO, while in photocatalytic reactions CH_4 was the carbon containing product.

The hydrogenation of carbon dioxide, which has been extensively studied in situ methods. We tried to map a simple reaction, the hydrogenation of CO_2 at the molecular level by studying it with different in situ techniques. The reaction was performed on a mesoporous NiO supported catalyst doped with controlled size 2D Pt nanoparticles. Based on the obtained results from the NAP-XPS (Near ambient X-ray Photoelectron spectroscopy) and DRIFTS methods and catalytic measurements, we deduced the mechanism of the reaction and the possible intermediates, and we obtained information on how the chemical composition of the surface changes under the reaction conditions.

The hydrogenation and methanation of CO_2 were carried out on spinel structures, too. Cobalt/manganese-oxide interface catalyst showed an outstanding activity and selectivity towards methane even at high temperatures. This unexpected finding is linked to the presence of a unique nanostructured Co/Mn(II)O with a surface composition of $Mn_{3.3}Co_{2.0}O_{4.7}$ formed after the pretreatment activation step. This hypothesis is proven by the combination of ex-situ XRD, TPR, HRTEM-ED, HAADF-EDX, and in-situ NAP-XPS and DRIFTS techniques. Phosphorus-loaded alumina supported nickel catalysts for CO_2 hydrogenation. $Ni/NiO/Ni_2P/Ni_5P_{12}/AlPO_4$ interfacial species were detected on the surface as active species on the used catalysts by X-ray photoelectron spectroscopy. The nickel enrichment in the surface layer presumable in Ni_2P/Ni_5P_{12} form is very likely according to the P 2p spectra and the authors assume that could be responsible for the enhanced catalytic activity. Surface phase transformation and catalytic reactions on Rh-modified 1D titanates (nanotubes and nanowires) were reviewed. It was concluded that the structure of support markedly influenced the activity of catalysts in CO_2 hydrogenation, H_2O + CO reaction, and ethanol transformation reactions.